Numerical studies on saltwater intrusion in a coastal aquifer in northwestern Germany

Tomas Feseker

Abstract Saltwater intrusion in coastal aquifers depends on the distribution of hydraulic properties, on the climate, and on human interference such as land reclamation. In order to analyze the key processes that control saltwater intrusion, a hypothetical steady-state salt distribution in a representative cross-section perpendicular to the coastline was calculated using a two-dimensional density-dependent solute transport model. The effects of changes in groundwater recharge, lowering of drainage levels, and a rising sea level on the shape and position of the freshwater/saltwater interface were modeled in separate simulations. The results show that the exchange of groundwater and surface water in the marsh areas is one of the key processes influencing saltwater intrusion. A rising sea level causes rapid progression of saltwater intrusion, whereas the drainage network compensates changes in groundwater recharge. The time scale of changes resulting from altered boundary conditions is on the order of decades and centuries, suggesting that the present-day salt distribution does not reflect a steady-state of equilibrium.

Résumé L'intrusion d'eau salée dans les aquifères côtiers dépend de la distribution des propriétés hydrauliques, du climat et de l'intervention humaine, telle que la mise en valeur des terres. Afin d'analyser les processus clés qui contrôlent l'intrusion saline, une distribution hypothétique du sel en régime permanent sur une section représentative perpendiculaire au littoral a été calculée, au moyen d'un modèle de transport de solutés en deux dimensions qui prend en compte les densités. Les effets des changements de la recharge des eaux souterraines, du rabattement des niveaux de drainage, et de la montée du niveau marin sur la forme et la position de l'interface entre l'eau douce et l'eau salée ont été modélisés dans des simulations différentes. Les résultats montrent que l'échange entre les eaux souterraines et les eaux de surface dans les zones marécageuses est l'un des processus clés influençant l'intrusion d'eau salée. Une élévation du niveau de la mer induit une progression rapide de l'intrusion d'eau salée, tandis que les changements de la recharge des eaux souterraines sont compensés par le réseau de drainage. L'échelle de temps des changements résultant de conditions aux limites changeantes est de l'ordre de décades et de siècles, ce qui suggère que la distribution actuelle du sel ne reflète pas l'équilibre d'un régime permanent.

Resumen La incursión de agua salada en acuíferos costeros depende de la distribución de propiedades hidráulicas, el clima, y la interferencia humana tal como recuperación de la tierra. Para analizar los procesos clave que controlan la incursión de agua salada se calculó una distribución hipotética de sal en régimen permanente en una sección transversal representativa perpendicular a la linea de costa usando un modelo de transporte de soluto en dos dimensiones dependiente de la densidad. Se elaboró un modelo con simulaciones separadas de los efectos de cambios en recarga de agua subterránea, disminución de niveles de drenaje, y de un nivel del mar ascendente en la forma y posición de la superficie de contacto agua dulce/agua salada. Los resultados muestran que el intercambio de agua subterránea y agua superficial en las áreas pantanosas es uno de los procesos clave que influencian la incursión de agua salada. El nivel de mar ascendente causa una progresión rápida de incursión de agua salada, mientras que los cambios en recarga de agua subterránea se compensan con la red de drenaje. La escala de tiempo de los cambios que resultan de alterar las condiciones limitantes es en el orden de décadas y siglos lo que sugiere que la distribución actual de sal no refleja un régimen permanente de equilibrio.

Received: 2 August 2004 / Accepted: 13 December 2006
Published online: 30 January 2007

T. Feseker (✉)
Geosciences,
Universität Bremen,
P.O. Box 330440, 28334, Bremen, Germany
e-mail: tomas.feseker@ifremer.fr

Present address:
T. Feseker
Ifremer Centre de Brest,
Géosciences Marines,
BP 70, 29280, Plouzané, France

Keywords Coastal aquifers · Groundwater/surface-water relations · Saltwater/freshwater relations · Numerical modeling · Germany

 DOI 10.1007/s10040-006-0151-z

Introduction

The coastal regions are the most densely populated areas in the world. Cohen et al. (1997) estimate that in 1994, more than one third of the world's population lived within 100 km of a coastline. At the same time, the coastal regions provide about one third of the world's ecosystem services and natural capital (Costanza et al. 1997). The growth of human settlements is accompanied by an increasing demand for water supply and excessive drainage for land reclamation purposes. Expected climate change will additionally influence the coastal groundwater system. As a consequence, the coastal groundwater resources are increasingly threatened by over-exploitation and pollution. The contamination of groundwater resources by seawater intrusion is already a major concern in many coastal aquifers (Bear et al. 1999; IHP/OHP 2002; Llamas and Custodio 2003). Therefore, understanding the effects of different water-management strategies such as drainage for land reclamation purposes, and the role of climate change is essential for the sustainable use of coastal groundwater resources.

The phenomenon of seawater intrusion in coastal aquifers was first observed by Badon Ghijben and Drabbe (1889) during the exploration of groundwater resources close to Amsterdam. Several years later, Herzberg (1901) described saline groundwater on German islands in the North Sea. Badon-Ghijben and Herzberg independently developed an equation that expresses the depth of the freshwater/saltwater interface below sea level as a function of the elevation of the water table above sea level:

$$h_s = \frac{\rho_f}{\rho_{sea} - \rho_f} h \qquad (1)$$

where h_s is the depth of the freshwater/saltwater interface below sea level, ρ_f is the density of freshwater, ρ_{sea} is the density of saltwater, and h is the elevation of the water table above sea level. Due to the density difference between freshwater and saltwater, the freshwater experiences a buoyancy force and floats on top of the saltwater. Consequently, saltwater intrusion is a natural process that results from the equilibration of pressures in the ocean and in the adjacent coastal aquifer. However, the assumption of a steady-state of equilibrium implies that Eq. (1) can greatly underestimate or overestimate the thickness of freshwater in the case of non-hydrostatic conditions (Izuka and Gingerich 1998). Furthermore, the presence of a brackish transition zone between saltwater and freshwater, which results from dispersive and diffusive mixing, is neglected by assuming a sharp interface.

While various case studies of seawater intrusion have been published in the past decades, only a few of them take into account climate change and anthropogenic impact. For example, the relationship between sea-level changes and the saltwater/freshwater interface has been described for aquifers in the North American coastal plain (Meisler et al. 1984), New Jersey (Navoy 1991; Lennon et al. 1986), Texas (Leatherman 1984), Israel (Melloul and Collin 2006), Greece (Lambrakis and Kallergis 2001), Belgium (Vandenbohede and Lebbe 2002), and The Netherlands (Oude Essink 1996, 2001a,b). Mahesha and Nagaraja (1996) discussed the general relationship between groundwater recharge and seawater intrusion applying the Ghyben-Herzberg equation, and Lambrakis (1998) studied the human impact and coastal groundwater resources on the island of Crete. More recently, Ranjan et al. (2006a,b) applied a numerical model based on the sharp interface assumption to analyze the effects of climate change and land use on coastal groundwater resources in Sri Lanka.

In order to investigate the dynamics of groundwater flow and geochemical processes within a typical northern European coastal aquifer in an integrated approach, a

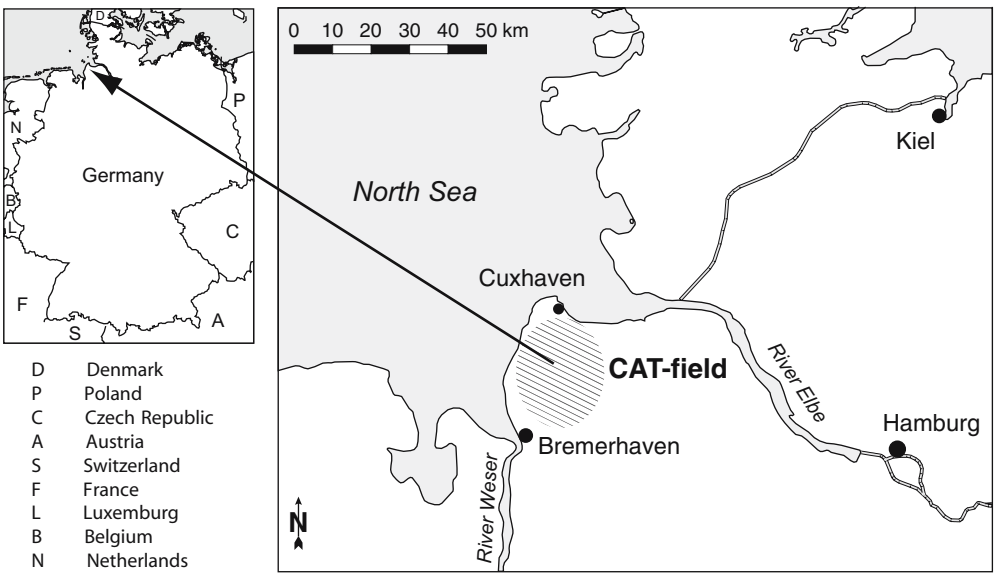

Fig. 1 The coastal aquifer test-field (*CAT-field*) is located in northwestern Germany, between the estuaries of the rivers *Elbe* and *Weser*

 DOI 10.1007/s10040-006-0151-z

coastal aquifer test-field (CAT-field) was established by the Leibnitz Institute for Applied Geosciences, Germany, in a representative region for the continental European North Sea coast. The CAT-Field is located in northwestern Germany, bordered by the estuaries of the rivers Elbe and Weser (Fig. 1). The results of geophysical investigations including seismic, gravity, and airborne electromagnetic surveys are published by Gabriel et al. (2003). Panteleit (2004) provided detailed analyses of the geochemical processes in the saltwater/freshwater transition zone. Fulda (2002) described the first numerical studies on the position of the freshwater/saltwater interface in the study area and discussed different possibilities of simulating drainage through constant head, constant concentration or constant flux boundary conditions.

This paper describes a hypothetical case study of the impact of climate change and changes in land use on the salt distribution in a coastal aquifer, inspired by the conditions found in the CAT-field at the German North Sea coast. The study focuses on the key processes that control the shape and position of the freshwater/saltwater interface. The role of possible changes in groundwater recharge, a rising sea level, and different drainage measures on the salt distribution are analyzed by applying a numerical model to simulate groundwater flow in a simplified representative cross-section perpendicular to the coast. Starting from a hypothetical steady-state scenario, four different simulations demonstrate how these boundary conditions affect the shape and extent of the saltwater wedge in the coastal aquifer.

In the following, all depths are given with respect to mean sea level (MSL). Elevations above MSL are expressed as positive values, while a negative sign marks a position below MSL. The coastline is taken as the origin of the horizontal axis, which is positive in a seaward direction. Consequently, the horizontal position of an inland point is denoted by a negative value.

Geology

The post-Permian geology of northwestern Germany is characterized by up to 500 m of sediments, which are underlain by the evaporitic deposits of the Upper Permian (Zechstein). As illustrated in Fig. 2, updoming of salt strongly affects the structure of the Tertiary and Quaternary sediments. Some salt domes even penetrate the Tertiary deposits and reach near-surface Quaternary sediments. The deposits of the Neogene and the Quaternary determine the hydrogeology.

The Neogene sediments consist of relatively uniformly distributed sequences of thick clay and sand layers (Fig. 2). Gravel and sand-rich onshore deposits of the Elster and Saale glaciation dominate the Quaternary sediments. Rapid variations of the sedimentation conditions during the Pleistocene caused a more heterogeneous distribution. In the study area, two buried Pleistocene glacial valleys have been identified which cut into the Tertiary sediments down to a depth of approximately 450 m (Haertlé 1983; Gabriel et al. 2003).

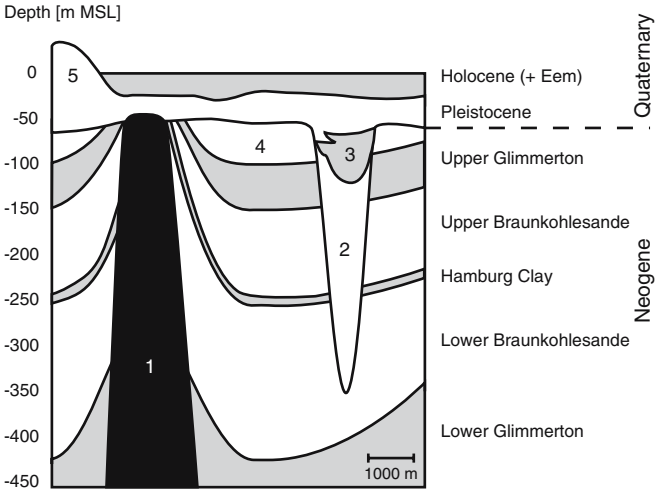

Fig. 2 Characteristic structures of the post-Permian geology in northwestern Germany: salt domes (*1*), buried valleys (*2*), Lauenburg Clay (*3*), Kaolinsande/Upper Miocene (*4*), geest (*5*; usually at 5–10 km from the coastline)

It is assumed that these valleys were eroded by meltwater during the Elster glaciation. However, the geological processes that formed the valleys are not yet fully understood. The main hypotheses are discussed, e.g., by Piotrowski (1997) and Huuse and Lykke-Andersen (2000). During the late Elster glaciation, the valleys were refilled with gravel, sand, silt, and clay, with grain sizes generally decreasing from the bottom to the top. The upper part of the channel filling commonly consists of a thick layer of clay (Lauenburg Clay) with intercalated silts and fine sands.

The glacigene onshore deposits outcrop at a distance of approximately 5–10 km from the coast and form slight ridges (geest) in the otherwise flat coastal plain. Towards the coastline, the Pleistocene deposits are covered by transgressive tidal flat sediments that are Eemian and Holocene in age, which interfinger with muds of brackish lagoonal type and with onshore peat deposits. The Holocene sequence commonly starts with a basal peat horizon. Different regressions and transgressions can be derived from intercalated layers of peat (Gerdes et al. 2003; Streif 2004). In the study area, the thickness of the Eemian sediments is approximately 3–5 m, while the thickness of the Holocene sequence ranges between 15 and 20 m (Sindowski 1979).

Hydrogeology

On a regional scale, two main aquifers can be distinguished in the study area (Haertlé 1983). The upper aquifer consists mainly of gravel and sand-rich sediments of the Pleistocene and includes fine and very fine-grained sands (Kaolinsande) that were deposited during the Pliocene and the Upper Miocene. The Quaternary sediments are generally characterized by excellent permeabilities, whereas the permeability of the Neogene deposits is medium to poor (Panteleit 2004). The thickness of the

 DOI 10.1007/s10040-006-0151-z

upper aquifer ranges between less than 50 m and more than 200 m within the Pleistocene erosion channels. Silt- and clay-rich sediments of the Middle and Upper Miocene (Upper Glimmerton) form the base of the upper aquifer. The lower aquifer is made up of sand-rich sediments of the Lower and Middle Miocene (Lower and Upper Braunkohlesande). Another thick clay layer (Lower Glimmerton) forms the base of the lower aquifer.

Based on pumping tests, Koschel and Lillich (1975) compiled a classification scheme describing the empirical relationship between grain-size distribution and hydraulic conductivity in aquifers in northwestern Germany. Applying this scheme to drilling logs, Haertlé (1983) concluded that the hydraulic resistance of the Upper Glimmerton separating the two aquifers is very large. Estimated values of its hydraulic conductivity are in the range of 1×10^{-9} m s^{-1} and 3×10^{-9} m s^{-1}. The piezometric heads at the base of the upper aquifer are between 2 and 6 m higher than at the top of the lower aquifer, causing downward leakage through the clay layer (Haertlé 1983). However, due to the thickness of the aquitard, the very low hydraulic conductivity, and the minor pressure gradient, the leakage flux does not exceed 10 mm year^{-1}. In the area of the deep Pleistocene valleys, the separating clay layer between the two aquifers was eroded such that there is only a single aquifer. However, Haertlé (1983) supposes that the Lauenburg Clay, which is commonly found at approximately the same depth as the Upper Glimmerton (Fig. 2), may act as a replacement and again led to a subdivision into two aquifers on a local scale.

The geest ridges are the most important groundwater recharge areas in the coastal region of northwestern Germany because the permeability of the sand-rich glacigene sediments is generally good and the distance from ground surface to the water table is greater than in the marsh areas. Due to extensive drainage for agricultural and land reclamation purposes, rather than recharge, a negative groundwater balance is expected in the marsh areas (Giesel and Schmidt 1978; Fulda 2002). The exchange of groundwater and surface water in the marsh areas is considered a key factor in the coastal groundwater system. Giesel and Schmidt (1978) showed that the pattern of groundwater flow can be modeled simply by describing recharge in the geest area and drainage in the marsh area as a function of the distance from ground surface to the water table. Using isotopic dating of water samples, Suckow (2001) calculated downward velocities between 1.2 and 1.3 m year^{-1}. Assuming reasonable values of porosity, this corresponds to groundwater recharge in the range of 350–400 mm year^{-1}. Based on surface-water budget calculations, Friedhoff (2001) estimates the net flux of groundwater into the drainage network at 120 mm year^{-1}.

As a result of the density difference between saltwater and freshwater, seawater intrudes from the North Sea into both the lower and the upper aquifer and forces the fresh groundwater upward. Electric conductivity measurements at observation wells (Haertlé 1983; Panteleit 2004) and airborne electromagnetic surveys (Repsold 1990; Gabriel et al. 2003) indicate that saltwater has intruded far into the upper aquifer. Close to the coastline, the groundwater in the upper aquifer is completely saline. At a distance of 4 km from the coastline, the freshwater/saltwater interface was found at depths of between 40 and 60 m below ground surface (Panteleit 2004), suggesting that the slope of the interface is very gentle. Further inland towards the geest, the slope increases significantly (Gabriel et al. 2003). In the vertical direction, the transition zone between freshwater and saltwater is usually restricted to a few meters (Panteleit 2004). Chemical analysis of groundwater samples show that other possible sources of salt beside the intrusion of seawater from the North Sea such as the mobilization of residual marine waters from deeper layers (Meinardi 1991) or the dissolution of halite from the underlying Permian salt, can be ruled out at least for the upper aquifer (Panteleit 2004). In the lower aquifer, the saltwater intrusion extends much further inland such that the groundwater in the lower aquifer is completely saline on a regional scale (Haertlé 1983). East of the study area, however, Haertlé (1983) observed that the lower parts of both aquifers are saline and the upper parts are fresh.

Method

The position and shape of the freshwater/saltwater interface depends on the hydraulic properties of the aquifer as well as on the boundary conditions such as the sea level, the rate of groundwater recharge, and the drainage levels. In case the saltwater intrusion is not at a steady-state of equilibrium, the distribution of salt in the aquifer at some initial stage and changes in the boundary conditions with time additionally influence the observed situation (cf. Oude Essink 2001b). Without this information, it is impossible to model field cases of saltwater intrusion. At present, the available data is insufficient for creating a model that accurately represents the pattern of groundwater flow and the distribution of salt in the study area. Moreover, it would not be possible to calibrate the model due to the lack of detailed observation data from deeper layers. Therefore, a conceptual model of a representative cross-section perpendicular to the coast was derived by simplifying the hydrogeological structure of the study area. This hypothetical aquifer possesses all characteristics of a typical coastal aquifer in northwestern Germany.

Conceptual model of a representative cross-section

As illustrated in Fig. 3, the conceptual model was limited to a cross-section of 10 km in length and reached to a depth of −120 m MSL. Only the upper aquifer was considered, assuming that leakage to the lower aquifer is negligible. Within the aquifer, two regions with different hydraulic properties are distinguished. The lower part from −120 to −60 m MSL represents the Upper Miocene sediments, which are characterized by medium permeability. The upper part of the aquifer (above −60 m MSL)

 DOI 10.1007/s10040-006-0151-z

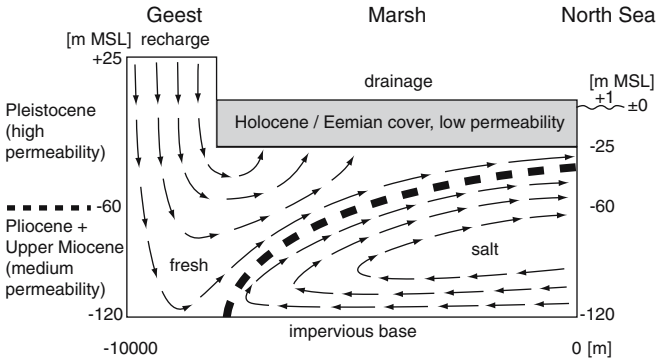

Fig. 3 Conceptual model of a representative cross-section through the upper aquifer. In the *marsh* region, the aquifer is overlain by a low-permeability cover layer, which represents the *Eemian* and *Holocene* deposits. To account for the different lithologies of the upper (*Pleistocene*) and lower (*Pliocene and Upper Miocene*) part of the aquifer, it is assumed that the hydraulic conductivity is significantly lower below a depth of *−60* m MSL. Groundwater recharge is limited to the geest ridge on the inland boundary of the cross-section. Saltwater intrudes into the aquifer from the seaward boundary along the impervious base and forces the fresh groundwater upward, where it is either drained of discharged into the *North Sea*

consists of highly permeable Pleistocene deposits. The aquifer outcrops at a distance of 8 km from the coast and forms a ridge 2 km wide, representing the geest. It is assumed that the inland boundary of the model domain coincides with the groundwater divide. In the marsh area, the topography is completely flat at an elevation of +1 m MSL. With the exception of the geest ridge, the entire aquifer is covered by a low-permeability layer 25 m thick, which represents the Eemian and Holocene deposits. Groundwater recharge only occurs in the geest area, whereas the water table in the marsh is controlled by drainage. In the conceptual model, each region is assumed to be homogenous.

Numerical model

A numerical model of the representative cross-section through the upper aquifer was created using the computer program SWIMMOC (Feseker 2004a). Based on the method of characteristics groundwater transport model MOC (Konikow and Bredehoeft 1978), relatively coarse grids can be used in SWIMMOC without numerical dispersion significantly affecting the transition zone between freshwater and saltwater. The program applies the concept of equivalent freshwater head to account for density differences:

$$h_f(z) = (z_{wt} - z)\frac{\rho}{\rho_f} + z \tag{2}$$

where $h_f(z)$ is the equivalent freshwater head at the depth z, z_{wt} is the elevation of the water table, ρ is the density, and ρ_f is the density of freshwater. As the equivalent freshwater head is a purely fictitious value that describes a saltwater head in terms of freshwater, it cannot be compared directly to values of hydraulic head measured in the field. The following equation describes the conversion from equivalent freshwater head to the hydraulic head that can be observed in the field, e.g., in a well:

$$h_{obs} = (h_f - z)\frac{\rho_f}{\rho} + z \tag{3}$$

where h_{obs} is the observed hydraulic head. The use of equivalent freshwater heads makes it necessary to add a buoyancy term to the vertical component of the flow equation:

$$S_s\frac{\partial h_f}{\partial t} = -K_x\frac{\partial^2 h_f}{\partial x^2} - K_z\frac{\partial}{\partial z}\left(\frac{\partial h_f}{\partial z} + \frac{\rho}{\rho_f} - 1\right) + W \tag{4}$$

where S_S is the specific storage, and K_X and K_Z are the horizontal and vertical hydraulic conductivities, respectively, and W is a source term. Concentration changes in time and space are described by the two-dimensional solute transport equation:

$$\begin{aligned}\frac{\partial(n_e c)}{\partial t} = {} & \frac{\partial}{\partial x}\left[n_e(D_{xx} + D_M)\frac{\partial c}{\partial x} + n_e D_{xz}\frac{\partial c}{\partial z}\right] \\ & + \frac{\partial}{\partial z}\left[n_e(D_{zz} + D_M)\frac{\partial c}{\partial z} + n_e D_{zx}\frac{\partial c}{\partial x}\right] \\ & - \frac{\partial(q_x c)}{\partial x} - \frac{\partial(q_z c)}{\partial z} + W c_W\end{aligned} \tag{5}$$

where n_e is the effective porosity, c is the concentration, D_{xx}, D_{zz}, D_{xz}, and D_{zx} are the components of the dispersion tensor, D_M is the coefficient of molecular diffusion, q_x and q_z are the horizontal and vertical components of specific flow, and c_W is the source concentration. Following the method of characteristics, the specific flow is calculated by solving the groundwater flow Eq. (4), and a particle tracking method is applied to calculate the concentration changes. Both steps are coupled bi-directionally via a linear equation of state, in which the density of groundwater is assumed to be directly proportional to the salinity, while all other factors influencing the density were neglected:

$$\rho = \rho_f + c\frac{\rho_{sea} - \rho_f}{c_{sea}} \tag{6}$$

where ρ_{sea} and c_{sea} are the density and salt concentration of seawater, respectively, which are used as reference values.

For the simulations presented here, the representative cross-section was discretized using an equidistant finite-differences grid consisting of 24 rows and 41 columns. The resulting grid cells were 250 m wide and 5 m high. As illustrated in Fig. 4, the model domain was subdivided into three subdomains, representing the Pleistocene and Pliocene/Upper Miocene parts of the aquifer and the Eemian/Holocene cover layer. The hydraulic properties of these subdomains are listed in Table 1. For all subdomains, an anisotropy ratio was assumed such that the hydraulic conductivity in the horizontal direction is ten times larger than in the vertical direction. The horizontal and vertical hydraulic conductivities of the Holocene/

 DOI 10.1007/s10040-006-0151-z

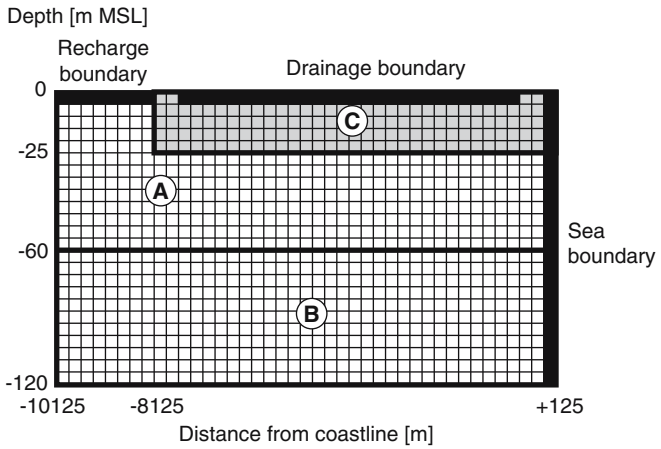

Fig. 4 Model grid, subdomains, and boundary conditions. The upper part of the aquifer (high permeability) was represented by subdomain *A*. Subdomain *B* described the lower part of the aquifer (lower permeability). The low-permeability cover layer was represented by subdomain *C*. All boundaries of the model domain were no-flow boundaries, unless a different boundary condition was defined (*black cells*). At the recharge boundary, groundwater recharge was simulated by means of a constant flux boundary condition which was applied to the outcrops of the upper aquifer (geest). At the drainage boundary, a head-dependent flux boundary condition represented drainage in the marsh region. The seaward boundary of the model domain was comprised of a prescribed fixed head (sea level) and a constant concentration (saltwater) boundary condition

Eemian cover layer (subdomain C) were derived from in-situ streambed hydraulic-conductivity measurements using a standpipe-method (Feseker 2004b). All remaining values reflect the grain-size composition of the sediments.

As discussed by Oude Essink (1996), appropriate values of longitudinal and transverse dispersivity for medium- and large-scale coastal aquifer solute transport models in The Netherlands and Belgium are on the order of centimeters or decimeters, which is significantly smaller than generally accepted values, especially for field studies in the USA. In order to account for the narrow transition zone between freshwater and saltwater that has been observed in the study area, the longitudinal and transverse dispersivities were set to 0.2 and 0.02 m, respectively, while molecular diffusion was neglected. Due to the time scale of the simulations, transient storage was not considered. Since the discharge of freshwater from the rivers Elbe and Weser into the North Sea dilutes the coastal seawater, a maximum saltwater density of 1,023 kg m^{-3} rather than the standard seawater value of 1,025 kg m^{-3} was used. The density of freshwater was set to 1,000 kg m^{-3}. The concentration values corresponding to freshwater density and maximum saltwater density are arbitrary. For convenience, a value of one was used in the context of this work to represent maximum saltwater concentration.

Three different types of boundary conditions were applied to simulate groundwater recharge, drainage, and the seaward boundary of the model domain (Fig. 4). Groundwater recharge in the geest area was represented by a constant flux (Neumann-condition) of freshwater across the upper border of the boundary cells. The boundary condition representing the North Sea at $x=0$ was a combination of a constant concentration and a prescribed head boundary condition (Dirichlet conditions):

$$c = c_{\mathrm{sea}} \tag{7}$$

$$h_{\mathrm{obs}}(t) = z_{\mathrm{sea}}(t) \tag{8}$$

where $z_{\mathrm{sea}}(t)$ is the sea level at the time t. While the concentration of the groundwater in the boundary cells was kept equal to the maximum saltwater concentration, the observed head may vary with time following a predefined function. Internally, SWIMMOC converts the observed head boundary condition to equivalent freshwater head:

$$h_{\mathrm{f}}(t) = [h_{\mathrm{obs}}(t) - z]\frac{\rho}{\rho_{\mathrm{f}}} + z \tag{9}$$

The exchange of water between the Holocene cover layer and a drainage network in the marsh area was

Table 1 The model domain was subdivided into three subdomains A, B, and C, which describe the two different parts of the aquifer and the cover layer

Model domains	Explanation
Subdomain A	
Age	Pleistocene
Lithology	Dominated by sand and gravel
Horizontal hydraulic conductivity	$K_x=1\times10^{-3}$ m s^{-1}
Vertical hydraulic conductivity	$K_x=1\times10^{-4}$ m s^{-1}
Effective porosity	$n_e=0.2$
Subdomain B	
Age	Upper Miocene + Pliocene
Lithology	Fine and very fine-grained sand with silt and clay layers
Horizontal hydraulic conductivity	$K_x=1\times10^{-4}$ m s^{-1}
Vertical hydraulic conductivity	$K_x=1\times10^{-5}$ m s^{-1}
Effective porosity	$n_e=0.2$
Subdomain C	
Age	Holocene + Eem
Lithology	Peat, clay, silt, fine sand
Horizontal hydraulic conductivity	$K_x=3\times10^{-6}$ m s^{-1}
Vertical hydraulic conductivity	$K_x=3\times10^{-7}$ m s^{-1}
Effective porosity	$n_e=0.15$

 DOI 10.1007/s10040-006-0151-z

Table 2 Boundary conditions used to obtain a steady-state position of the freshwater/saltwater interface

Boundary conditions	Explanation
Recharge boundary condition	
Type	Constant flux
Flux concentration	Freshwater
Volumetric flux	1.2×10^{-8} m s^{-1} (≈380 mm year^{-1})
Sea boundary condition	
Type	Constant concentration and prescribed observed hydraulic head
Concentration	Saltwater
Observed hydraulic head	0 m MSL
Drainage boundary condition	
Type	Head-dependent flux
Surface-water level	+1 m MSL (= ground surface)
Surface-water bottom	+1 m MSL
Streambed hydraulic conductivity	3×10^{-7} m s^{-1}
Streambed thickness	1 m

implemented as a head-dependent flux boundary condition (Cauchy condition). This drainage boundary condition was defined by the thickness and vertical hydraulic conductivity of the drainage channel streambed and its elevation relative to the boundary cell. The volumetric flux across the upper border of these boundary cells depends on the hydraulic gradient between the surface water and the groundwater:

$$q_L = \left[(H_s - z_{bottom})\frac{\rho_s}{\rho_f} + z_{bottom} - h_f\right]\frac{K_L}{m_L} \quad (10)$$

where q_L is the specific leakage flux across the semi-pervious layer, H_s is the surface water level, z_{bottom} is the elevation of the bottom of the surface water body, ρ_s is the density of the surface water, and K_L and m_L are the vertical hydraulic conductivity and the thickness of the semi-pervious layer. In the case of the water level in the drainage channel being lower than the equivalent freshwater head at the base of the streambed, exfiltration of groundwater from the aquifer into the drainage channel occurs. On the other hand, a downward hydraulic gradient leads to the infiltration of freshwater from the drainage channel into the aquifer. If the freshwater head in the aquifer falls below the base of the semi-pervious layer, the leakage flux into the aquifer becomes independent of the hydraulic gradient between the surface water and the aquifer. In this case, the leakage flux is controlled by the distance between the equivalent freshwater head at the bottom of the surface water and the base of the semi-pervious layer (cf. Kinzelbach and Rausch 1995):

$$q_L = \left[(H_s - z_{bottom})\frac{\rho_s}{\rho_f} + m_L\right]\frac{K_L}{m_L} \quad (11)$$

The effects of changing boundary conditions on the position and shape of the freshwater/saltwater interface can only be analyzed if the initial situation reflects a steady-state of equilibrium. Otherwise, it would be impossible to distinguish between the influence of the altered boundary condition and changes resulting from unsteady initial conditions. Therefore, a hypothetical steady-state position of the freshwater/saltwater interface was calculated through continuous simulation using constant boundary conditions (Table 2), including a 'natural' drainage level which is equal to ground surface. The resulting steady-state situation was used as the initial condition in the subsequent analysis of the influence of the different boundary conditions on the salt distribution in the aquifer. All results shown here were obtained using a head convergence criterion of 1×10^{-5} m and four particles per cell.

Results

Using the constant boundary conditions listed in Table 2, a balance of solute mass flux into and out of the model domain was reached after a simulated time of 3,000 years. Figure 5 illustrates how the solute mass accumulated in the model aquifer during the progression of the saltwater intrusion until the total salt concentration in the model domain approached 35%. The concentration distribution at equilibrium is shown in Fig. 6. In the following, the isoline, indicating a seawater fraction of 0.5, is taken as the freshwater/saltwater interface. Close to the coast, the interface is found at a depth of approximately −30 m

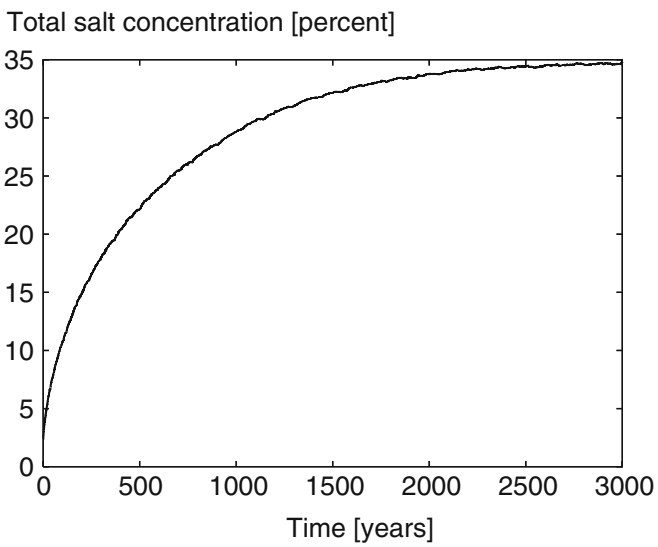

Fig. 5 Steady-state was reached after a simulated time of approximately 3,000 years when the total salt concentration in the model domain approached 35%

 DOI 10.1007/s10040-006-0151-z

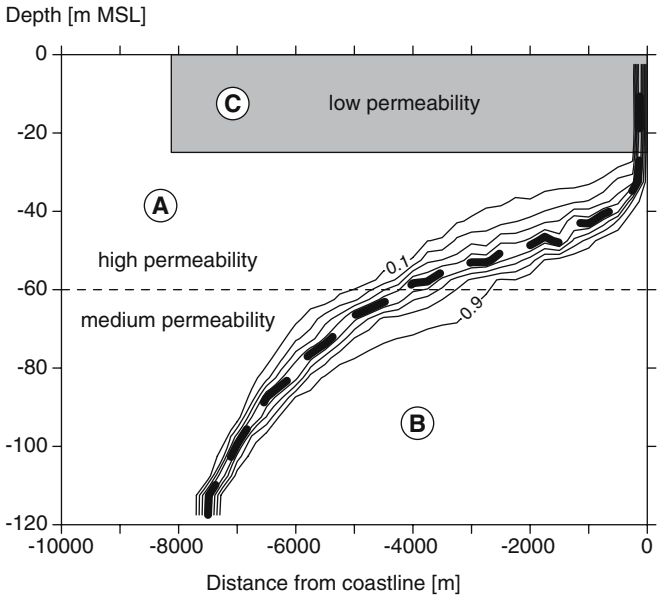

Fig. 6 The hypothetical steady-state distribution of salt is illustrated by lines of equal concentration, with labels indicating the fraction of seawater. The position of the freshwater/saltwater interface (0.5 seawater) is marked by the *thick-dashed line*. *A* subdomain A; *B* subdomain B; *C* subdomain C

MSL, sloping gently inland. The slope increases significantly at a distance of about 5,000 m from the coastline after the depth of the medium permeability subdomain (B) has been reached. The transition zone is widest at the border between the subdomains A and B, suggesting that the widening is associated with the corresponding change in hydraulic properties. Except for the sea boundary cells, the concentration of the groundwater in the entire area of subdomain C is lower than 0.1 seawater concentration. A large fraction of the recharged groundwater was drained in the marsh area close to the geest ridge, while infiltration from the drainage network into the Eemian/Holocene cover layer occurred in those boundary cells that were closer than 2,000 m to the coast (Fig. 7). The net drainage flux in the marsh area was approximately 3.17×10^{-9} m s^{-1} or 100 mm year^{-1}, which is about 93% of the total groundwater recharge.

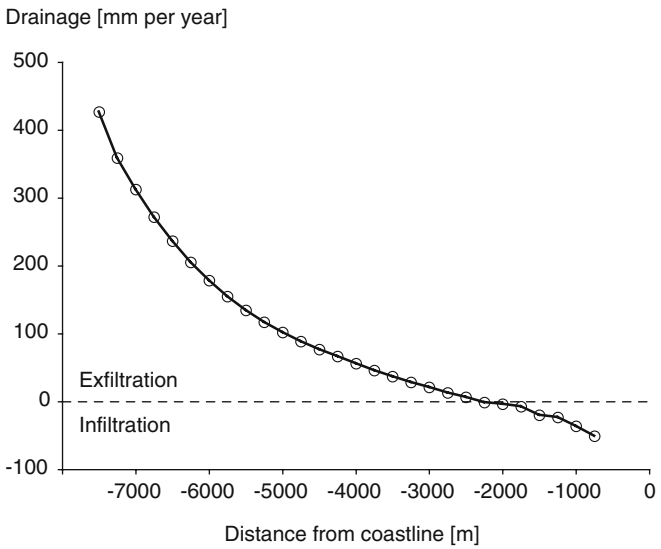

Fig. 7 Drainage rates for the hypothetical steady-state condition. Positive values show exfiltration of groundwater from the aquifer into the drainage channels while negative values indicate infiltration of surface water from the drainage channels into the aquifer

Sensitivity analysis

In order to analyze the effects of groundwater recharge, drainage, and a rising sea level on the shape and position of the freshwater/saltwater interface, the corresponding boundary conditions were changed one at a time and the influence on the groundwater system was modeled in separate simulations. For all scenarios, the hypothetical steady-state solution described above was used as the initial condition.

Groundwater recharge

The sensitivity of the freshwater/saltwater interface to changes in groundwater recharge was investigated in two simulations. For the first simulation, the recharge flux in the geest area was reduced from 1.2×10^{-8} to 8×10^{-9} m s^{-1}, which corresponds to approximately 250 mm year^{-1}. The modeled positions of the interface for this scenario after 100, 200, 300, 400, and 500 years of simulated time are shown in Fig. 8. The decrease in groundwater recharge resulted in progression of the saltwater intrusion at the base of the aquifer, while changes in the position of the interface were negligible above a depth of about −60 m MSL. Significant salinization of near-surface groundwater did not occur. The changes in the position of the interface

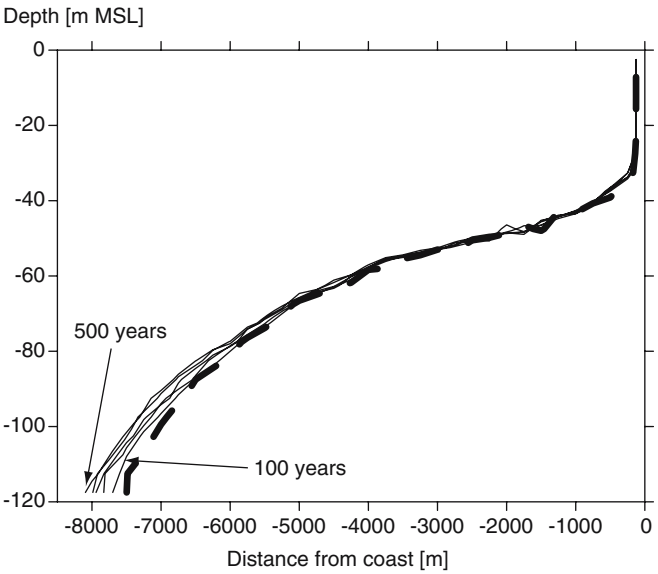

Fig. 8 Groundwater recharge was reduced by one third. The *thin lines* mark the position of the freshwater/saltwater interface after *100–500* years of simulated time at increments of 100. The *thick-dashed line* shows the initial position of the interface, which was at equilibrium with the higher recharge rate

 DOI 10.1007/s10040-006-0151-z

became less rapid in the course of the simulation as the system approached a steady-state equilibrium.

The second simulation used an increased recharge rate of 1.6×10^{-8} m s^{-1} or approximately 500 mm year^{-1}. The simulation results for 100, 200, 300, 400, and 500 years of simulated time are illustrated in Fig. 9. Increasing the groundwater recharge caused a retreat of the saltwater wedge at the base of the aquifer, while the shape and position of the freshwater/saltwater interface remained unchanged above a depth of approximately −60 m MSL. The higher groundwater recharge flux led to a retreat of the saltwater wedge at the base of the aquifer, while no significant changes in the position of the freshwater/saltwater interface could be observed above approximately −60 m MSL. The salinity of near-surface groundwater was negligible. As the system adjusted to the altered boundary condition, the changes became less rapid.

Comparing the rates of drainage for the two different scenarios with changed recharge flux to the drainage rates for the steady-state situation (Fig. 10) shows that changes in the recharge boundary condition were compensated for by drainage in the marsh area close to the geest. An increase of recharge led to an increase of drainage, whereas a lower recharge flux was reflected by lower drainage. Closer to the coastline, the drainage flux rates remained almost unchanged, such that infiltration of water from the drainage network into the Eemian/Holocene cover layer occurred in both scenarios. After 500 years of reduced recharge, the net drainage flux was approximately 2×10^{-9} m s^{-1} or 72 mm year^{-1}, which corresponds to 89% of the recharged groundwater. The net drainage flux resulting from 500 years of increased groundwater recharge was about 4.3×10^{-9} m s^{-1} or 144 mm year^{-1}, corresponding to 94% of the recharged groundwater.

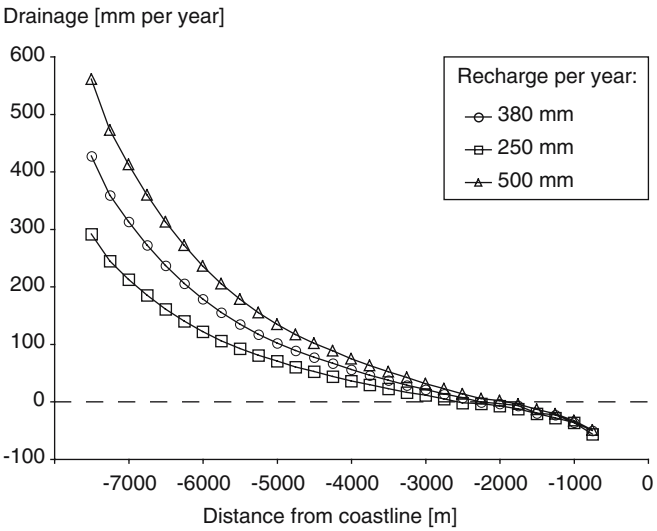

Fig. 10 Comparison of the drainage rates for the hypothetical steady-state situation (*circles*), the scenario with reduced recharge (*squares*), and the scenario with increased recharge (*triangles*) after 500 years of simulated time

Drainage

The effect of drainage on the salt distribution in the aquifer was analyzed through a simulation with the drainage level lowered from +1 to +0.5 m MSL. The calculated positions of the freshwater/saltwater interface for 100, 200, 300, 400, and 500 years of simulated time are shown in Fig. 11. The lower drainage level resulted in a rapid general raise of the interface. Closer than 2,000 m from the coastline, the interface approached the base of the Eemian/Holocene cover layer asymptotically, indicating that some salinization of the near surface groundwater may occur. In the

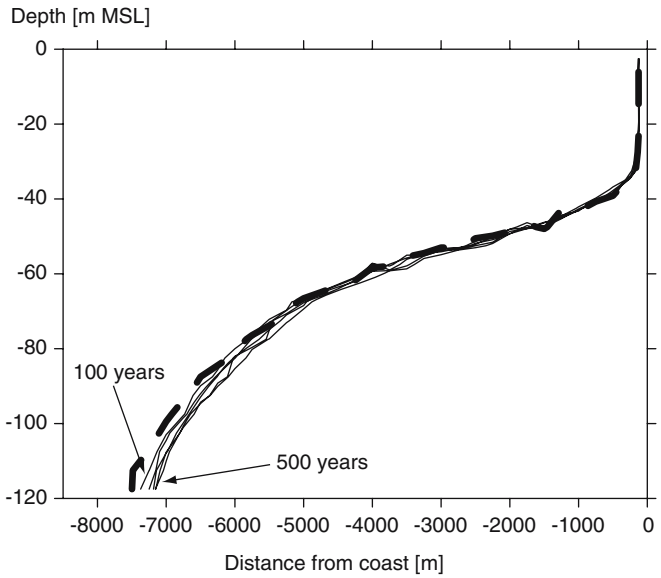

Fig. 9 Groundwater recharge was increased by one third. The position of the freshwater/saltwater interface after *100–500 years* of simulated time at increments of 100 is illustrated by the *thin lines*. The *thick-dashed line* shows the initial position of the interface, which was at equilibrium with the lower recharge rate

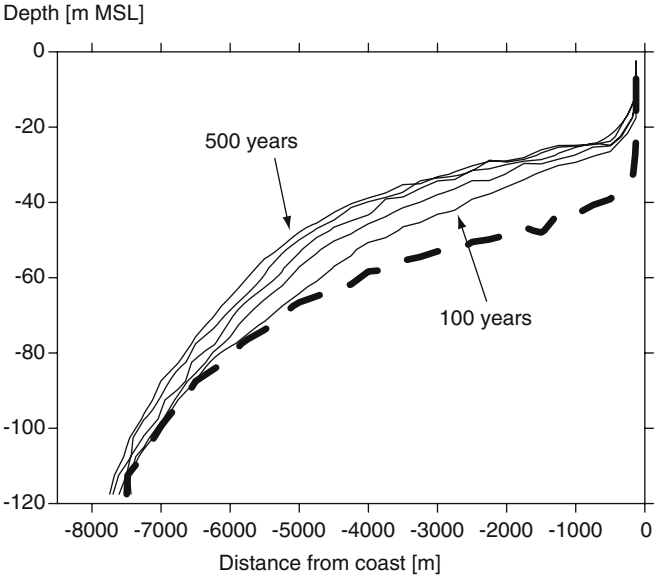

Fig. 11 The drainage level was lowered from +1 to +0.5 m MSL. The *thin lines* show the position of the freshwater/saltwater interface after a simulated time of *100–500 years* at increments of 100. The *thick-dashed line* represents the initial position of the interface at equilibrium with the higher drainage level

 DOI 10.1007/s10040-006-0151-z

course of the simulation, the rate of change became less as the system adjusted to the altered boundary condition.

Sea-level rise

The IPCC projections of global sea level rise from 1990 to 2100 lie in the range of 0.11 to 0.77 m (Cubasch et al. 2001). In order to analyze the influence of a rising sea level on the position of the freshwater/saltwater interface, a sea level rise of 0.5 m per century is simulated, starting from the modeled steady-state of equilibrium including drainage. The model results for 50, 100, 150, 200, and 250 years of simulated time are illustrated in Fig. 12. The rising sea level causes a rapid increase of the groundwater salinity in the Eemian/Holocene cover layer close to the shoreline.

Figure 13 shows a comparison of the drainage rates for the hypothetical steady-state situation, the scenario with lowered drainage level, and the scenario with rising sea level. High drainage rates close to the geest area indicate that large quantities of groundwater were exfiltrated into the drainage network in all scenarios. On the other hand, infiltration of surface water into the Eemian/Holocene cover layer close to the coastline was reduced to a minimum in the scenario with lowered drainage level, and completely abolished in the scenario with rising sea level. The lowered drainage level led to a net drainage flux of 3.67×10^{-9} m s^{-1} or 116 mm year^{-1}, which is 107% of the groundwater recharge. The net drainage flux in the marsh area resulting from the rising sea level was 5×10^{-9} m s^{-1} or 158 mm year^{-1}, corresponding to 145% of the groundwater recharge.

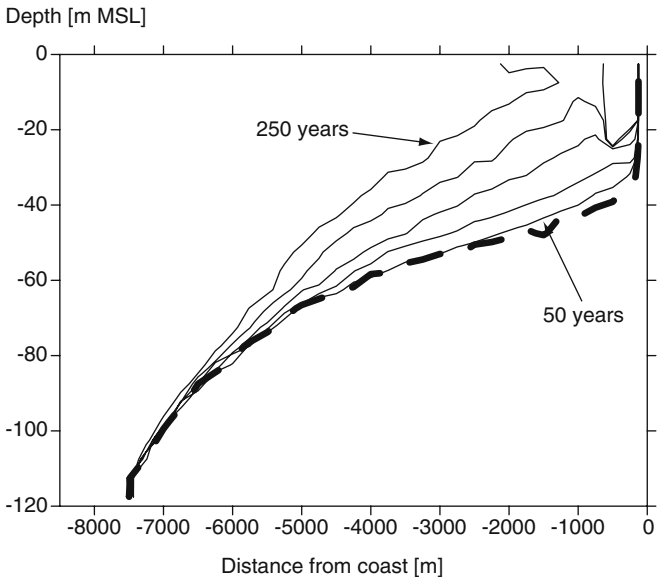

Fig. 12 The sea level is rising at a rate of 0.5 m per century. The *thin lines* mark the position of the freshwater/saltwater interface after *50–250 years* of simulated time at increments of 50. The *thick-dashed line* shows the initial position of the interface, which is at equilibrium with a sea level of 0 m MSL

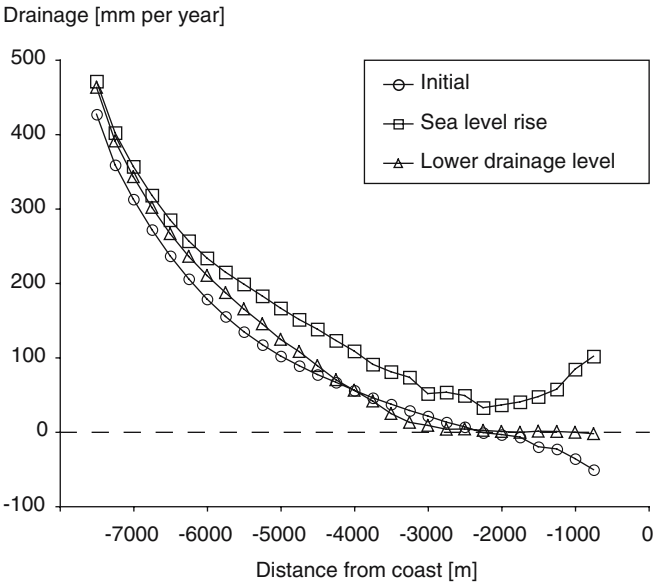

Fig. 13 Comparison of the drainage rates for the hypothetical steady-state situation (*circles*), the scenario with a sea level rise (*squares*), and the scenario with a lowered drainage level (*triangles*) after 250 and 500 years of simulated time with changed boundary conditions, respectively

Impact on total salt concentration

The impact on the total salt concentration within the model domain varies considerably in the four different test scenarios (Fig. 14). The changes in groundwater recharge that were simulated in the first two scenarios have only a little effect on the amount of salt in the hypothetical aquifer. However, even after a simulated time of 500 years with unchanged boundary conditions, the salt concentration is still changing slowly, reflecting that the system has not yet reached a stable equilibrium. As the total salt concentration in the model aquifer augments from initially 35% to more than 46% within 500 years following the change of the boundary condition, the impact of lowering the drainage level in the third scenario is much more

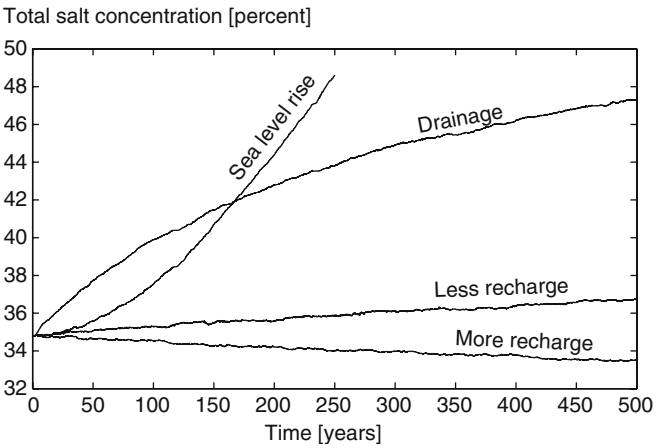

Fig. 14 Comparison of the impact of the studied boundary conditions (*sea level rise*, *drainage*, *less recharge*, and *more recharge*) on the percentage of total salt concentration in the model domain over a span of 500 years

DOI 10.1007/s10040-006-0151-z

significant. From the convex-upward shape of the concentration curve for this scenario can be seen that the system slowly adjusts to the changed boundary condition, but does not reach equilibrium after 500 years of simulated time. The constantly rising sea level has the most severe effect on the coastal groundwater resources. During the first 150 years, the concave-upward shape of the concentration curve shows how the model adjusts from the constant sea level in the hypothetical steady-state scenario to the rising sea level. Subsequently, the salt concentration increases linearly and exceeds 48% after only 250 years of simulated time.

Discussion

Observations of the salt distribution (Repsold 1990; Gabriel et al. 2003; Panteleit 2004) in the coastal aquifer show that the present extent of saltwater intrusion is considerably larger than in the hypothetical steady-state situation. In reality, the saltwater/freshwater interface in the marsh areas is found less deep than in the hypothetical steady-state, which is most likely related to the drainage measures that are applied in the study area. The sharpness of the freshwater/saltwater interface in the vertical direction was well reproduced by the numerical model. The horizontal widening of the transition zone associated with the change in hydraulic properties between the model subdomains A and B (Fig. 6) may be the result of unstable density-dependent flow due to heterogeneity as described by Simmons et al. (2001).

The time scale of changes resulting from altered boundary conditions is on the order of decades and centuries, which agrees with numerical simulations of the dynamics of the freshwater/saltwater interface in coastal aquifers in Belgium (Vandenbohede and Lebbe 2002) and Greece (Lambrakis and Kallergis 2001). Oude Essink (2001b) states that saltwater intrusion in coastal aquifers in The Netherlands is not at a steady-state equilibrium, but constantly progressing. The slow reaction of the interface in the numerical simulations presented here suggests that the same conclusion applies to the coastal aquifers in northwestern Germany.

Simulating the evolution of a freshwater lens in the Belgian coastal plain, Vandenbohede and Lebbe (2002) observed that the modeled salt distribution was much more sensitive to changes in the drainage levels than to changes in the hydraulic conductivities, whereas the hydraulic conductivities seemed to control the time scale of the simulated processes. The sensitivity of the simulation results to the hydraulic properties of the aquifer and the cover layer was not analyzed in the study presented here. However, it seems feasible that the nature of the processes described will be the same for slightly varied hydraulic properties.

The drainage rates that were calculated in the different simulations range from 72 to 158 mm year^{-1} and compare well with the value of 120 mm year^{-1}, which was estimated by Friedhoff (2001). The graphs of the drainage rates at different distances from the coastline (Figs. 7, 10, and 13) provide a detailed insight into the effects of drainage on groundwater flow. They illustrate that the exchange of groundwater and surface water in the marsh area is one of the key processes determining the position of the freshwater/saltwater interface coastal aquifers in northern Germany and confirm the results presented by Giesel and Schmidt (1978) and Fulda (2002).

The distance from the coastline to the geest ridges was not considered in the sensitivity analyses of the model. However, the simulations with different rates of groundwater recharge in the geest area suggest that smaller or greater distances would mainly lead to a different distribution of drainage rates in the marsh area. If the geest was further away from the coastline, the slopes of the drainage curves shown in Fig. 10 would be more gentle, while the curves would be steeper if the geest was closer to the coastline. In neither case would the shape of the freshwater/saltwater interface differ significantly from the hypothetical test case. Analogously, the main effects of different widths of the geest area would be due to the change of the surface area that is subject to groundwater recharge and thus correspond to different rates of groundwater recharge.

Conclusions

The numerical simulations of the four scenarios with altered boundary conditions showed that:

- Variations in groundwater recharge of 30% were largely compensated by the drainage measures and had only minor impact on the position of the freshwater/saltwater interface.
- The drainage level controlled the depth of the freshwater/saltwater interface in the marsh area. Lowering the drainage level by 0.5 m caused a rise of the interface of about 20 m and lead to a significant increase of the salt concentration in the model domain.
- A constantly rising sea level resulted in a linear increase of the salt load in the model domain with successive salinification of the marsh area from the coastline towards the geest.

Considering the sluggish adjustment of the coastal groundwater system to the imposed boundary changes, it is very likely that the present-day situation does not reflect a steady-state equilibrium of saltwater intrusion, drainage, and recharge. Consequently, saltwater intrusion may progress and salinization of soils close to the coastline may increase, even if groundwater recharge does not decrease, the sea level does not rise, and the drainage levels are not lowered. On the other hand, the same time scale must be expected for countermeasures to take effect. Therefore, further investigations of the dynamics of saltwater intrusion based on more detailed data are important to ensure a sustainable use of coastal groundwater resources.

 DOI 10.1007/s10040-006-0151-z

Acknowledgements This work was funded by the University of Bremen, Germany, as part of the interdisciplinary research project "Lebensraum Nordseeküste". The manuscript was reviewed by H. Kooi, L.C. Lebbe, and G.H.P. Oude Essink. Their constructive critiques and suggestions lead to significant improvements and are gratefully acknowledged.

References

Badon Ghijben W, Drabbe J (1889) Nota in verband met de voorgenomen putboring nabij Amsterdam [Remarks concerning the accomplished drilling close to Amsterdam], Tijdschrift van het Koninklijk Instituut voor Ingenieurs, The Hague, pp 8–22

Bear J, Cheng AH-D, Sorek S, Ouzar D, Herrera I (1999) Seawater intrusion in coastal aquifers: concepts, methods and practices. Kluwer, Dordrecht

Cohen JE, Small C, Mellinger A, Gallup J, Sachs J (1997) Estimates of coastal populations. Science 278(2):1211–1212

Costanza R, d'Arge R, de Groot R, Farber S, Grasso M, Hannon B, Limburg K, Naeem S, O'Neill R, Paruelo J, Raskin RG, Sutton P, van den Belt M (1997) The value of the world's ecosystem services and natural capital. Nature 387:253–260

Cubasch U, Dai X, Ding Y, Griggs DJ, Hewitson B, Houghton JT, Isaksen I, Karl T, McFarland M, Meleshko VP, Mitchell JFB, Noguer M, Nyenzi BS, Oppenheimer M, Penner JE, Pollonais S, Stocker T, Trenberth KE (2001) Technical summary. In: Houghton JT, Ding Y, Griggs DJ, Noguer M, van der Linden PJ, Dai X, Maskell K, Johnson CA (eds) Climate change 2001: the scientific basis. Contribution of Working Group I to the third assessment report of the intergovernmental panel on climate change. Cambridge University Press, Cambridge

Feseker T (2004a) A saltwater intrusion model based on the method of characteristics: user's guide to SWIMMOC, Universität Bremen, published online at http://www.geochemie.uni-bremen.de/downloads/swimmoc/. Cited 8 January 2007

Feseker T (2004b) Numerical studies on groundwater flow in coastal aquifers, PhD Thesis, Universität Bremen, Germany

Friedhoff T (2001) Wasserhaushaltsuntersuchungen im tidebeeinflussten Einzugsgebiet der Medem (Land Hadeln) [Water budget investigations in the tidal catchment area of the Medem (Land Hadeln)], Hochschule Bremen, Germany

Fulda C (2002) Numerische Studien zur Salz-/Süßwasserverteilung im Rahmen der Cuxhavener Forschungsbohrung [Numerical studies on the freshwater/saltwater distribution regarding the scientific drilling project in Cuxhaven], Mitteilungen der Deutschen Geophysikalischen Gesellschaft, vol II, pp 10–26

Gabriel G, Kirsch R, Siemon B, Wiederhold H (2003) Geophysical investigation of buried Pleistocene subglacial valleys in northern Germany. J Appl Geophys 53(4):159–180

Gerdes G, Petzelberger BEM, Scholz-Böttcher BM, Streif H (2003) The record of climatic change in the geological archives of shallow marine, coastal, and adjacent lowland areas of northern Germany. Quat Sci Rev 22(1):101–124

Giesel W, Schmidt G (1978) Grundwasserumsatz zwischen Geest und Marsch [Groundwater exchange between geest and marsh]. Geol Jahrb C(23):53–62

Haertlé T (1983) Geologisch-hydrogeologische und hydrochemische Untersuchungen im niedersächsischen Bereich der Unteren Elbe [Geological-hydrogeological and hydrochemical investigations in the Lower Saxonian area of the Lower Elbe], PhD Thesis, Albert-Ludwigs-Universität Freiburg, Germany

Herzberg A (1901) Die Wasserversorgung einiger Nordseebäder [The water supply of some spas at the North Sea]. J Gasbeleuch Wasserversorg 44(44):815–819

Huuse M, Lykke-Andersen H (2000) Overdeepened Quaternary valleys in the eastern Danish North Sea: morphology and origin. Quat Sci Rev 19(12):1233–1253

IHP/OHP (2002) Proceedings of the international symposium on low-lying coastal areas: hydrology and integrated coastal zone management. IHP/OHP Berichte 13:219–224

Izuka SK, Gingerich SB (1998) Estimation of the depth to the fresh-water/salt-water interface from vertical head gradients in wells in coastal and inland aquifers. Hydrogeol J 6(3):365–373

Kinzelbach W, Rausch R (1995) Grundwassermodellierung [Groundwater modeling]. Borntraeger, Berlin

Konikow LF, Bredehoeft JD (1978) Computer model of two-dimensional solute transport and dispersion in ground water. In: Techniques of water-resources investigations, Book 7, Chap. C2, US Geol Surv, Reston, VA

Koschel H, Lillich W (1975) Berechnung und Kartendarstellung der Ergiebigkeit von Typbrunnen zur Kennzeichnung des Entnahmepotentials von Lockergesteinsaquiferen [Calculation and mapping of the productiveness of wells to characterize the potential productiveness of sedimentary aquifers]. Dtsch Gewässerkdl Mitt 19(6):146–149

Lambrakis NJ (1998) The impact of human activities in the Malia coastal area (Crete) on groundwater quality. Environ Geol 36(1):87–92

Lambrakis N, Kallergis G (2001) Reaction of subsurface coastal aquifers to climate and land use changes in Greece: modelling of groundwater refreshening patterns under natural recharge conditions. J Hydrol 245(1–4):19–31

Leatherman SP (1984) Coastal geomorphic responses to sea level rise: Galveston Bay, Texas. In: Barth MC, Titus JG (eds) Greenhouse effect and sea level rise: a challenge for this generation. Reinhold, New York, pp 151–178

Lennon GP, Wisniewski GM, Yoshioka GA (1986) Impact of increased river salinity on New Jersey aquifers. In: Hull CHJ, Titus JG (eds) Greenhouse effect, sea level rise, and salinity in the Delaware Estuary. US EPA and Delaware River Basin Commission, Washington, DC, pp 40–54

Llamas R, Custodio E (2003) Intensive use of groundwater: challenges and opportunities. Balkema, Rotterdam

Mahesha A, Nagaraja SH (1996) Effect of natural recharge on sea water intrusion in coastal aquifers. J Hydrol 174(3–4):211–220

Meinardi CR (1991) The origin of brackish groundwater in the lower parts of The Netherlands. In: De Breuck W(eds) Hydrogeology of salt water intrusion: a selection of SWIM papers

Meisler H, Leahy PP, Knobel LL (1984) Effect of eustatic sea-level changes on saltwater-freshwater in the northern Atlantic coastal plain. US Geol Surv Water Suppl Pap 2255

Melloul A, Collin M (2006) Hydrogeological changes in coastal aquifers due to sea level rise. Ocean Coast Manage 49(5–6):281–297

Navoy AS (1991) Aquifer-estuary interaction and vulnerability of groundwater supplies to sea level rise-driven saltwater intrusion, PhD Thesis, Pennsylvania State University, USA

Oude Essink GHP (1996) Impact of sea level rise on groundwater flow regimes, PhD Thesis, Delft University of Technology, The Netherlands

Oude Essink GHP (2001a) Salt water intrusion in a three-dimensional groundwater system in The Netherlands: a numerical study. Transp Porous Media 43(1):137–158

Oude Essink GHP (2001b) Saltwater intrusion in 3D large-scale aquifers: a Dutch case. Phys Chem Earth, Part B Hydrol Oceans Atmos 26(4):337–344

Panteleit B (2004) Geochemical processes in the saltwater/freshwater transition zone. PhD Thesis, Universität Bremen, Germany

Piotrowski JA (1997) Subglacial hydrology in northwestern Germany during the last glaciation: groundwater flow, tunnel valleys, and hydrological cycles. Quat Sci Rev 16(2):169–185

Ranjan P, Kazama S, Sawamoto M (2006a) Effects of climate and land use changes on groundwater resources in coastal aquifers. J Environ Manage 80(1):25–35

Ranjan P, Kazama S, Sawamoto M (2006b) Effects of climate change on coastal fresh groundwater resources. Glob Environ Change 80:25–35

Repsold H (1990) Geoelektrische Untersuchungen zur Bestimmung der Süßwasser-/Salzwassergrenze im Gebiet zwischen Cuxhaven und Stade [Geoelectrical investigations to determine the freshwater/saltwater interface in the area between Cuxhaven and Stade]. Geol Jahrb C(56):3–37

Simmons TC, Fenstemaker TR, Sharp JM Jr (2001) Variable-density groundwater flow and solute transport in heterogeneous porous media: approaches, resolutions and future challenges. J Contam Hydrol 52(1–4):245–275

Sindowski K-H (1979) Zwischen Jadebusen und Unterelbe [Between Jadebusen and Unterelbe], Sammlung geologischer Führer, vol 66. Borntraeger, Berlin

Streif H (2004) Sedimentary record of Pleistocene and Holocene marine inundations along the North Sea coast of Lower Saxony, Germany. Quat Int 112(1):3–28

Suckow A (2001) Isotopenhydrologische Multiparameterstudien im Rahmen des Forschungsschwerpunktes Grundwasser: erste Ergebnisse [Multi-parameter studies on hydrological isotopes in the framework of the exploratory focus groundwater: first results], Tagung der Arbeitsgemeinschaft Nordwestdeutscher Geologen, Bremerhaven, Germany

Vandenbohede A, Lebbe L (2002) Numerical modelling and hydrochemical characterisation of a fresh-water lens in the Belgian coastal plain. Hydrogeol J 10:576–586

 DOI 10.1007/s10040-006-0151-z